DETERMINISTIC AND STOCHASTIC SURROGATE MODELS FOR A SLOWLY DRIVEN FAST OSCILLATOR

MARCEL OLIVER AND MARC TIOFACK KENFACK

Abstract. It has long been known that the excitation of fast motion in certain two-scale dynamical systems is linked to the singularity structure in complex time of the slow variables. We demonstrate, in the context of a fast harmonic oscillator forced by one component of the Lorenz 1963 model, that this principle can be used to construct time-discrete surrogate models by numerically extracting approximate locations and residues of complex poles via Adaptive Antoulas–Andersen (AAA) rational interpolation and feeding this information into the known "connection formula" to compute the resulting fast amplitude. Despite small but nonnegligible local errors, the surrogate model maintains excellent accuracy over very long times. In addition, we observe that the long-time behavior of fast energy offers a continuous-time analog of Gottwald and Melbourne's 2004 "0–1 test for chaos" – the asymptotic growth rate of the energy in the oscillator can discern whether or not the forcing function is chaotic.

1. Introduction

Two-scale dynamical systems often possess adiabatic invariants, such as the energy in the fast subsystem, which are preserved over long periods of time [29]. Typical examples are the spring pendulum with a stiff spring, or balance in geophysical fluid flow [41, 26]. Here, we aim to model and quantify the residual transfer of energy in and out of the fast subsystem using information on only the slow components of the dynamics.

The slow subsystem can often be constructed as a divergent asymptotic series in the scale separation parameter [44] but it is rarely an exact invariant of the full system [15, 16, 25]. Optimal truncation of the asymptotic series, however, typically yields exponentially small exchange of energy over exponentially long times [8, 30, 31, 35]. Careful asymptotic analysis in the context of low-dimensional models reveals that the exchange of energy between slow and fast subsystems can be linked to the presence of complex-time singularities in the slow components and explicit expressions for the transfer amplitude can be derived [9, 39, 40, 42]. The interpretation of the transfer process as a Stokes phenomenon [6, 32] classifies it as a time-discrete phenomenon in an asymptotic sense.

We take a new look at this old problem from the following angle: (i) What can we say about the statistical behavior of the fast compartment when the slow motion is chaotic, and (ii) can we use this knowledge to construct a surrogate model that operates purely on the slow time scale? We answer these questions

Date: January 21, 2024.

2020 *Mathematics Subject Classification.* Primary 34M40; Secondary 41A20, 34E13.

Key words and phrases. Balance, forced oscillator, Stokes phenomenon, rational interpolation, chaos.

in one of the simplest possible proof-of-concept settings: a single fast harmonic oscillator driven by one of the components of Lorenz's 1963 model. We do not consider any feedback from the oscillator onto the Lorenz dynamics but rather consider the Lorenz system as a generator for a quasi-random sequence of complex-time singularities. This is the simplest configuration in which we can study these questions without being encumbered by the details of the model as would be the case for models of intermediate complexity or in infinite dimensions.

Our first observation is that the dynamics of the fast amplitude is extremely well approximated by a random walk that approaches Brownian motion in a long-time scaling when the Lorenz dynamics is chaotic and appears quasi-periodic when the Lorenz dynamics is in a periodic regime, a dichotomy which is the continuous-time analog of the "0–1 test for chaos" of Gottwald and Melbourne [17, 19]. A related dichotomy in a continuous-time dynamical system was observed by Alvarez-Socorro *et al.* [2] in the context of studying a pinning-depinning transition in front propagation.

Our second finding is that the full dynamics can be replicated extremely accurately, path-wise, by a surrogate model where the necessary information on the transition amplitudes is extracted from the slow motion by applying rational interpolation to the numerical trajectory and using the resulting approximate complex-time poles as input to the "connection formula" which describes the jump in fast amplitude across a Stokes line. Therefore, the surrogate model takes the form of a discrete walk in the complex plane for the complex amplitude of the fast motion. As such, the evolution of the modulus of the fast amplitude depends on the relative phase of each additional step, which is essentially, but not entirely, uncorrelated between subsequent steps. Thus, stochastic surrogate models can be constructed by randomizing the choice of phase.

Our main tool is the Adaptive Antoulas–Anderson ("AAA") algorithm for rational interpolation, introduced by Nakatsukasa *et al.* [27], which provides us with a robust estimator for the location of the complex-time poles and their residues of the slow dynamics. The AAA algorithm has been applied to a variety of different problems [28], including, recently, the study of Stokes phenomena similar to what is done here [10, 24].

This paper is structured as follows. In Section 2, we review the asymptotic theory for high-order fast-slow splitting of the forced oscillator. This can be done in many ways; our presentation is in a form that easily generalizes to more complicated situations. Section 3 is a review of the derivation of the connection formula via matched asymptotics. Again, this material is classical, but we provide details for the convenience of the reader and, in particular, point out that the dynamics of the fast amplitude can be written as a discrete walk in the complex plane. Section 4 introduces the full coupled system. By direct numerical simulation, we observe that the solution in the fast phase space performs approximately a discrete random walk. We link this observation to the 0–1 test for chaos. Section 5 gives an overview of rational interpolation and, specifically, the AAA algorithm. We then test the accuracy of the AAA approximation in conjunction with the asymptotic connection formula. In Section 6, we introduce the surrogate model, replacing the fast components of the coupled system with the AAA-estimator coupled with the

connection formula. Section 7 looks at phase randomization for the complex transition amplitude to account for the inherent uncertainty in knowing precise phase information. The paper concludes with a brief discussion and outlook.

2. The slow expansion

We consider a fast harmonic oscillator with a forcing function $g(t)$ that varies slowly relative to the period of oscillation,

$$\varepsilon^2\,\ddot{q}(t) + q(t) = g(t)\,, \tag{1}$$

with ε a small parameter. The solution can be written as the linear combination of the general solution to the homogeneous equation, which is spanned by $\exp(\pm \mathrm{i}t/\varepsilon)$, and a particular solution to the inhomogeneous problem. Let us assume that the particular solution can be written as an asymptotic series in ε. To leading order, the position simply follows the forcing, i.e., $q_0(t) = g(t)$. Higher-order terms are easily constructed, for example by repeated integration-by-parts of the variations-of-constant formula (see, e.g., [40]) or, as sketched below, by direct expansion. The latter approach is equivalent but generalizes more easily to systems and nonlinear equations.

Let us write $p = \varepsilon\,\dot{q}$,

$$\boldsymbol{v} = \begin{pmatrix} q \\ p \end{pmatrix}, \qquad \boldsymbol{g} = \begin{pmatrix} 0 \\ g \end{pmatrix}, \qquad \text{and } J = \begin{pmatrix} 0 & -1 \\ 1 & 0 \end{pmatrix}. \tag{2}$$

Then (1) takes the form

$$\varepsilon\,\dot{\boldsymbol{v}} + J\boldsymbol{v} = \boldsymbol{g}\,. \tag{3}$$

Seeking a slow solution, a solution that is slaved to $\boldsymbol{g}$ to order ε^N,

$$\boldsymbol{v}^N_{\text{slow}} = \sum_{n=0}^{N} \varepsilon^n\,\boldsymbol{v}_n(\boldsymbol{g}) \tag{4}$$

and writing $\boldsymbol{v}^N_{\text{fast}} = \boldsymbol{v} - \boldsymbol{v}^N_{\text{slow}}$, we find, by direct computation, that

$$\dot{\boldsymbol{v}}^N_{\text{fast}} = -\frac{1}{\varepsilon} J\boldsymbol{v}^N_{\text{fast}} + \frac{1}{\varepsilon}\left[\boldsymbol{g} - J\boldsymbol{v}_0(\boldsymbol{g})\right] - \sum_{n=0}^{N-1} \varepsilon^n \left[J\boldsymbol{v}_{n+1}(\boldsymbol{g}) + \mathrm{D}\boldsymbol{v}_n(\boldsymbol{g})\dot{\boldsymbol{g}}\right] + \mathcal{O}(\varepsilon^N)\,, \tag{5}$$

where D denotes the total derivative. As the first term is skew, it does not change the fast energy

$$E^N_{\text{fast}} = \|\boldsymbol{v}^N_{\text{fast}}\|^2\,. \tag{6}$$

Overall, the fast energy remains invariant to $\mathcal{O}(\varepsilon^N)$ when the intermediate terms in (5) drop out, which is the case when

$$\boldsymbol{v}_n = -J^{n+1}\,\frac{\mathrm{d}^n \boldsymbol{g}}{\mathrm{d}t^n} \tag{7}$$

for $n = 0, \ldots, N$. Thus, unless g is entire, the series (4) does not converge as $N \to \infty$. Indeed, when g is analytic on the strip $|\mathrm{Im}\,t| < r$, we have the Cauchy estimate

$$|g^{(n)}(t)| \le M\,\frac{n!}{r^n} \lesssim \sqrt{n}\left(\frac{n}{r\mathrm{e}}\right)^n \quad \text{with} \quad M = \sup_{|\mathrm{Im}\,z|<r} |g(z)|\,, \tag{8}$$

the second bound due to Stirling's approximation. When g has poles, this bound is essentially sharp, so that an optimal truncation of the series is achieved by choosing $N \sim r/\varepsilon$ (see, e.g., [11]), and

$$\varepsilon^N \, |g^{(N)}(t)| \lesssim \frac{1}{\sqrt{\varepsilon}} \, \mathrm{e}^{-\frac{r}{\varepsilon}} \, . \tag{9}$$

As we shall compute in the next section, and already noted in [40], the remainder of the series is larger, by a factor of $\sqrt{\varepsilon}$, than bound (9) on the last included term, but is still exponentially small. We also see that the influence of the remainder on the evolution of the fast energy is strongest when t is closest to a complex-time singularity of g, which is the time when the bounds above saturate. A careful analysis is given in the next section.

3. Matched asymptotics

Let us first assume that $g(t)$ has a single pair of simple poles, i.e.

$$g(t) = \frac{a}{t - t_\star} + \text{entire} + \text{c.c.} \tag{10}$$

where the entire remainder gives rise to a converging slow expansion, thus does not contribute to the excitation of fast motion, and there is a complex conjugate contribution since g is assumed to be real-valued. To begin, we neglect all but the first term on the right of (10).

Away from the pole at $t = t_\star$, the solution to (1) can be approximated by a superposition of the general solution to the harmonic oscillator and the leading order of the slow expansion, i.e.,

$$q(t) = A \, \mathrm{e}^{\mathrm{i}t/\varepsilon} + B \, \mathrm{e}^{-\mathrm{i}t/\varepsilon} + \frac{a}{t - t_\star} + O(\varepsilon) \tag{11}$$

for constants A and B to be determined later.

Near $t = t_\star$, this outer solution breaks down. A solution in the inner region is obtained by introducing scaled variables

$$\tau = \frac{t - t_\star}{\varepsilon} \quad \text{and} \quad \phi(\tau) = \frac{\varepsilon \, q(t)}{a} \, , \tag{12}$$

so that (1) reads

$$\phi'' + \phi = \frac{1}{\tau} \, , \tag{13}$$

where the superscript prime denotes differentiation with respect to τ. A formal solution is given by

$$\phi(\tau) = \frac{1}{2\mathrm{i}} \left[\mathrm{e}^{-\mathrm{i}\tau} \, E_1(-\mathrm{i}\tau) - \mathrm{e}^{\mathrm{i}\tau} \, E_1(\mathrm{i}\tau) \right] \tag{14}$$

where

$$E_1(z) = \int_z^\infty \frac{\mathrm{e}^{-1}}{t} \, \mathrm{d}t \tag{15}$$

is known as the *exponential integral*, as can be verified by direct computation. This solution is valid in any region of the complex plane where the right-hand side of (14) is analytic. Since E_1 has a logarithmic singularity at the origin, we need to make an appropriate choice of the associated branch cut. Assuming, without loss of generality, that $\operatorname{Im} t_\star > 0$, we wish to obtain a solution that is valid in the half plane $\{\operatorname{Im} \tau < 0\}$. Placing the branch cut of $E_1(z)$ onto the negative imaginary axis and working in the right half plane $\operatorname{Re} z > 0$, we observe that the argument of the second

exponential integral in (14) is always in the required half-plane. When $\tau = x - 0\mathrm{i}$ with $x < 0$, the argument of the first exponential integral is away from the branch cut, so can be moved into the right half plane by continuity. As $E_1(z) \sim \mathrm{e}^{-z}/z$ for $|\arg(z)| < \frac{3\pi}{2}$ as $|z| \to \infty$ [1, equation 5.1.51], this implies $E_1(\mathrm{i}\tau) \sim \mathrm{e}^{-\mathrm{i}\tau}/(\mathrm{i}\tau)$ and $E_1(-\mathrm{i}\tau) \sim \mathrm{e}^{\mathrm{i}\tau}/(-\mathrm{i}\tau)$, so that

$$\phi(\tau) \sim \frac{1}{\tau} \quad \text{for } \tau < 0\,. \tag{16}$$

When $\tau = x - 0\mathrm{i}$ with $x < 0$, the argument of the first exponential integral, $z = -\mathrm{i}\tau$, crosses over into the left half plane along the branch cut, and we need to use the identity

$$E_1(-\mathrm{i}(\tau - 0\mathrm{i})) = E_1(-\mathrm{i}\tau + 0) + 2\pi\mathrm{i}\,. \tag{17}$$

Then $E_1(-\mathrm{i}\tau) \sim \mathrm{e}^{\mathrm{i}\tau}/(-\mathrm{i}\tau) + 2\pi\mathrm{i}$ and $E_1(\mathrm{i}\tau) \sim \mathrm{e}^{-\mathrm{i}\tau}/(\mathrm{i}\tau)$, so that

$$\phi(\tau) = \frac{1}{\tau} + \pi\,\mathrm{e}^{-\mathrm{i}\tau} \quad \text{for } \tau > 0\,. \tag{18}$$

Matching the inner expansions (16) and (18) with the outer expansion (11) in an intermediate asymptotic regime gives $A = B = 0$ for $\operatorname{Re} t \ll 0$, resp. $A = 0$ (consistent with the expectation that there are no exponentially large terms) and

$$B = \frac{\pi\, a}{\varepsilon}\,\mathrm{e}^{\mathrm{i}t_\star/\varepsilon} \tag{19}$$

for $\operatorname{Re} t \gg 0$. Taking into account the contribution from the complex conjugate pole at $\bar{t}_\star$, we see that, as t crosses the "Stokes line" between the two poles, the oscillatory contribution

$$q_{\mathrm{fast}} \sim \frac{2\pi}{\varepsilon}\operatorname{Re}\bigl[a\,\mathrm{e}^{\mathrm{i}(t_\star - t)/\varepsilon}\bigr] \tag{20}$$

as $\varepsilon \to 0$ is "switched on", here again with the convention that $\operatorname{Im} t_\star > 0$ so that the fast contribution is exponentially small in ε.

This expression agrees with that of Vanneste [40, equation 3.6], who performed a careful analytic and numerical study on a single such emission event and found that the predicted asymptotic connection amplitude is in very good agreement with numerics, even for moderately small values of ε. He also demonstrated that the growth of fast amplitude in the inner region follows the profile of an error function. Here, however, we are not interested in the local details of a single emission event, but rather look for the cumulative effect of many events. Seen from the long time scale, each event contributes a discrete jump to the fast energy.

Let us thus assume that $g(t)$ has m pairs of complex conjugate simple poles with residues a_i and locations t_i with the convention that $\operatorname{Im} t_i > 0$, for $i = 1, \dots, m$, as well as their complex conjugate residues and locations. Identifying the amplitude of the vector $\boldsymbol{v}_{\mathrm{fast}} = (q_{\mathrm{fast}}, p_{\mathrm{fast}})$ with a point in the complex plane, (20) shows that each pair of complex conjugate poles contribute a complex connection amplitude

$$B_i = \frac{2\pi}{\varepsilon}\,a_i\,\mathrm{e}^{\mathrm{i}t_i/\varepsilon}\,. \tag{21}$$

The overall complex amplitude after crossing m Stokes lines is given by linear superposition, i.e.,

$$B(m) = \sum_{i=1}^{m} B_i\,. \tag{22}$$

Thus, the dynamics of the fast amplitude can be described as a discrete walk in the complex plane, each step exponentially small in ε and linked to the complex-time

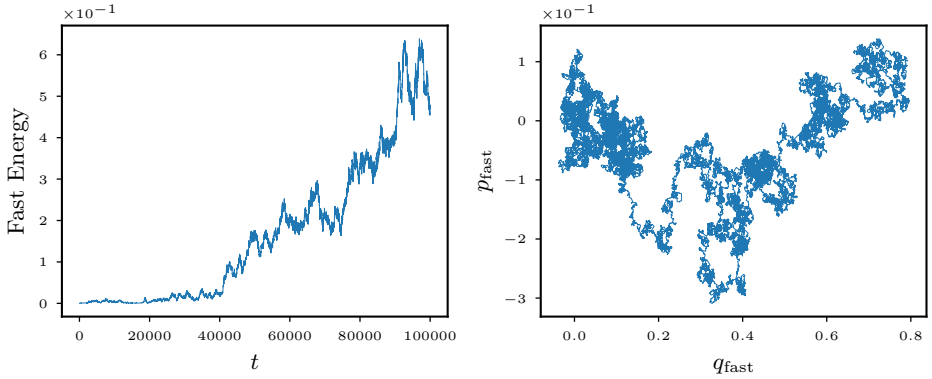

FIGURE 1. Fast oscillator driven by the Lorenz system in the chaotic regime with standard parameters $b = \frac{8}{3}$, $r = 28$, and $\sigma = 10$. We take $\varepsilon = 0.01$ and diagnose to order $N = 16$.

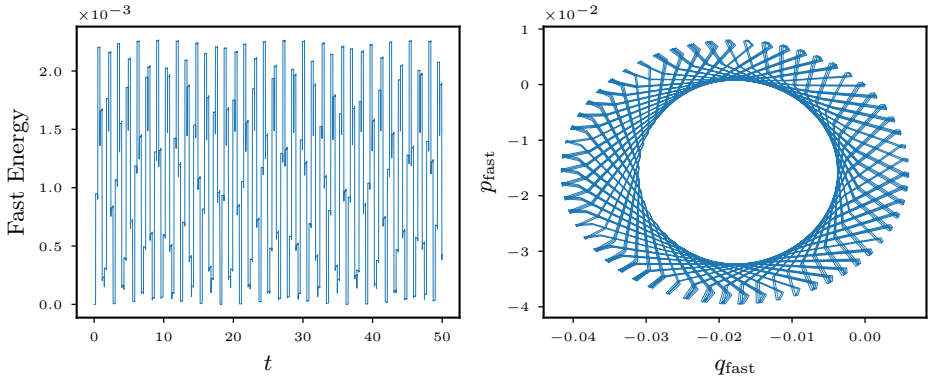

FIGURE 2. Fast oscillator driven by the Lorenz system in the periodic regime, here point A1 of [12] where $b = \frac{8}{3}$, $r = 402$, and $\sigma = 302$. We take $\varepsilon = 0.001$ and diagnose to order $N = 11$.

poles of g via (21). In the following, we are interested in the long-time asymptotics as $m \to \infty$.

4. Periodic vs. chaotic forcing

We employ the Lorenz 1963 model [23] as a driver for the forced oscillator equation (1). Originally derived by truncating the equations for Rayleigh–Bénard convection to lowest harmonics, the system is now a standard test case for concepts involving low-dimensional chaos. It reads

$$\dot{x} = \sigma(y - x)\,, \tag{23a}$$

$$\dot{y} = rx - y - xz\,, \tag{23b}$$

$$\dot{z} = xy - \tfrac{8}{3}z\,. \tag{23c}$$

In our context, the singularity structure of solutions on the attractor is crucial. Foias *et al.* [14] have shown that the attractor has an uniform radius of real analyticity, i.e., the singularities remain bounded away from the real time axis. A formal power count shows that if there are poles, they should be expected to be simple in x and of second order in y and z. Viswanath and Şahutoğlu [43] show that there are indeed solutions of this type, albeit with corrections given by logarithmic psi-series ("quasi-poles"). It remains open whether all singularities are locally of this type. Webb [45] has shown that the singularity structure of solutions to the Lorenz equations can be approximated via rational interpolation. Moreover, he found that the singularities are located close to the time at which the z-component has a local maximum. Thus, even though the Lorenz system is not known to strictly fit into the framework laid out in Section 3, its singularity structure appears to be close enough to make it an interesting test case.

We choose to drive the oscillator with the z-component of the Lorenz system, i.e. $g(t) = z(t)$. We first initialize the Lorenz system arbitrarily and run forward in time until the orbit is practically on the attractor. Then we initialize the oscillator in an optimally slow state via expression (4). Its coefficients (7) are computed via repeated analytic differentiation of the Lorenz equations, a task that is easily performed by computer algebra. The optimal order truncation N was determined empirically. The coupled system is then evolved forward in time.

As diagnostics, we plot the fast energy as given by (6). It shows clear jumps which, as we shall see later, are associated with complex-time singularities of $z(t)$. We also plot a Poincaré section of the orbit of $\boldsymbol{v}^N_{\text{fast}}$ which is obtained by sampling $\boldsymbol{v}^N_{\text{fast}}(t)$ at integer multiples of the fast period. For the standard values of the Lorenz parameters where the motion on the attractor is chaotic, the samples of the phase point are performing a pseudo-random walk in the fast phase space, see Fig. 1 where it is evident that the fast energy, on average, is growing in time.

When the parameters for the Lorenz system are changed so that the attractor is a single periodic orbit, the fast phase point follows a quasi-periodic motion and the fast energy remains bounded (Fig. 2).

This dichotomy is reminiscent of the "0–1 test for chaos" of Gottwald and Melbourne [17, 19]. The test asks whether a given, for simplicity infinite, scalar time series g_n is "regular" or "chaotic". The time series is used to drive the discrete-time dynamical system

$$p_{n+1} = p_n + g_n \cos(cn)\,, \tag{24a}$$

$$q_{n+1} = q_n + g_n \sin(cn)\,, \tag{24b}$$

for some fixed frequency parameter c. From there, one computes the *mean square displacement*

$$\mathrm{MSD}(n) = \lim_{N\to\infty} \sum_{j=1}^{N} \frac{|p_{j+n} - p_j|^2 + |q_{j+n} - q_j|^2}{N}\,. \tag{25}$$

Under mild assumptions, the *asymptotic growth rate* exists and generically takes one of two values:

$$K = \lim_{n\to\infty} \frac{\log \mathrm{MSD}(n)}{\log n} = \begin{cases} 0 & \text{iff } g_n \text{ regular}\,, \\ 1 & \text{iff } g_n \text{ chaotic}\,. \end{cases} \tag{26}$$

In the exceptional case when g_n is periodic and the frequency c is resonant, secular growth, corresponding to a quadratic increase of the mean square displacement is possible. A rigorous justification of this behavior is given in [18].

Here, we note that the 0–1 test is actually a discrete version of the driven harmonic oscillator: Writing (1) in co-rotating coordinates and discretizing with the explicit Euler scheme of unit step size gives (24).

5. Numerical detection of poles: The AAA algorithm

To link the behavior seen in the previous section with the singularity structure of the forcing function g, we need to continue the numerical solution, which is known only for a discrete set of real t, into the complex plane. The problem of analytic continuation is ill posed (see, e.g., [36]), but can be stabilized by implicit or explicit regularization. One such algorithm is the Adaptive Antoulas–Anderson (AAA) method, first introduced by Nakatsukasa *et al.* [27] and found to perform extremely well for the problem of analytic continuation [37]. Even though a complete theoretical analysis remains open, the observed excellent performance makes it the algorithm of choice for our purposes.

The starting point for the AAA algorithm is the barycentric rational interpolation formula [33, 34] for function values $f_1, \dots, f_m$ given on support points $z_1, \dots, z_m$,

$$r(z) = \frac{n(z)}{d(z)} = \sum_{k=1}^{m} \frac{w_k\, f(z_k)}{z - z_k} \Big/ \sum_{k=1}^{m} \frac{w_k}{z - z_k}\,. \tag{27}$$

The weights $w_1, \dots, w_m$ are arbitrary at this point, but non-zero. Continuously extending the function at the support points, we see that $r(z_k) = f_k$ for $k = 1, \dots, m$. The poles of r lie elsewhere; they can be computed efficiently by solving a generalized eigenvalue problem [22, 27]. The barycentric interpolation formula has excellent numerical stability. However, the global behavior of the interpolant, in particular the singular set, depend greatly on the choice of the weights and may be very unstable as a function of the data.

There are various strategies for choosing the weights [4, 5, 13]. In particular, Antoulas and Anderson [3] proposed to consider the rational *approximation* problem for sample points $\Gamma = \{z_1, \dots, z_M\}$ with sample values $f_1, \dots, f_M$ and select a subset $\Gamma_m \subset \Gamma$ with $m \ll M$ as support points on which the barycentric formula interpolates, then optimize the weights by solving the least-squares problem

$$\text{minimize } \|fd - n\|_{\Gamma\setminus\Gamma_m} \quad \text{subject to } \|w\|_m = 1\,, \tag{28}$$

where $\|\cdot\|_{\Gamma\setminus\Gamma_m}$ is the discrete 2-norm on the set of sample points which are not interpolation support points and $\|\cdot\|_m$ is the discrete 2-norm on m-vectors. This problem can be solved efficiently by singular value decomposition. However, the question remains how large m should be and how to choose the set Γ_m.

AAA uses a greedy selection procedure: start with a minimal set of support points Γ_m, solve the optimization problem, and check if the overall approximation error is acceptable. If it is not, pick the sample point with the largest pointwise error, add it to Γ_m, and repeat. This procedure typically converges very fast, e.g. root-exponentially even for functions with branch points [38].

Fig. 3 shows an approximation to the location of the poles of the function $g(t) = \operatorname{sech}(t)$, which is the standard example in [40], using the AAA algorithm on 50 equidistant real sample points in the interval $[-15, 15]$ with the restriction $m \leq$

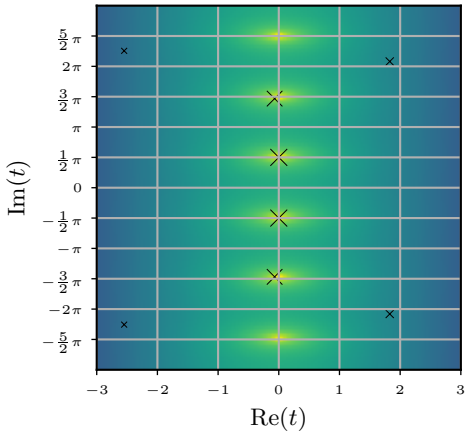

FIGURE 3. AAA-estimate of the location of the poles of sech(t).

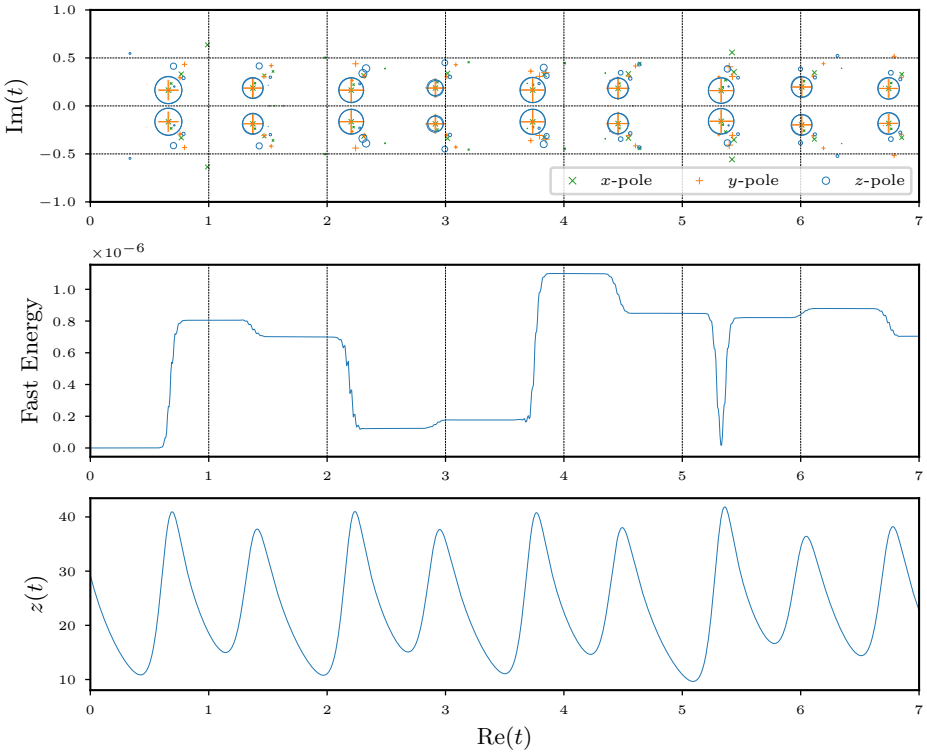

FIGURE 4. Approximation of the singularities of the Lorenz system via AAA rational approximation with $M = 1000$ sample points in the interval $[0, 7]$ (top), the corresponding evolution of fast energy of the forced oscillator with $\varepsilon = 0.01$ (middle), and the z-component of the Lorenz system driving the oscillator (bottom).

$m_{\max} = 9$. The colored background indicates the modulus of the true function, crosses indicate the estimated locations of the poles. The pair of poles closest to the real axis is reproduced with good accuracy, the location of the second pair is already slightly inaccurate, and further out, the estimates are completely off. The figure also shows that AAA does not impose any symmetries on the results, even when the data has an axis of symmetry.

For our purposes, this behavior is perfectly acceptable, as it is only the poles close to the real axis that matter. To put some numbers on this statement: on the $g(t) = \operatorname{sech}(t)$ test case with $\varepsilon = \frac{1}{4}$, certainly not a very small number, the asymptotic formula (21) applied with the exact values for the two innermost pairs of poles coincides with an estimate by direct numerical simulation, where the fast energy is diagnosed to order $N = 15$, up to a relative error of 0.00003 %. Using only the innermost pair of poles, accuracy drops to 0.0004 %. Replacing exact pole locations and residues with a AAA estimate based on 50 sample points, accuracy is "only" 0.001 %; in this setting, using more than one pair of AAA poles will not help. Increasing the number of sample points given to the AAA algorithm from 50 to 100, accuracy improves to 0.0002 %, apparently compensating some of the error of the connection formula. In this case, even though in this case the contribution from the second pole is fairly accurate, it does not help to improve the error, but neither does it hurt to include these contributions or even include the contributions from all further AAA poles.

One concern when using AAA is the possible emergence of spurious poles with a residue of order machine precision or poles so close together that they almost cancel each other out, which are called Froissart doublets [27]. These poles do not matter here as they do not contribute substantially to the connection amplitude (21) when the contributions of all poles are summed up. However, as we shall see later, when breaking up the forcing function into smaller pieces, the AAA approximation may produce poles that are close to the real axis, but outside of the sampling interval. These poles must be removed, for else they will contribute large spurious connection amplitudes.

For the Lorenz model, the singularity structure is conjectured to consist of complex conjugate pairs of branch points [43, 45]. The AAA approximation, on the other hand, will always construct a sequence of simple poles, as can be seen in Fig. 4 (upper panel). Here, the discrete pole with the largest residue is located close to the presumed branch point, with further poles of smaller residue further out in the complex plane, indicating the possible location of a branch cut. Close inspection of the data shows that each of the dominant poles in the y- and z-components close to the real axis is actually a pair of twin poles with almost the same location and residue. This is consistent with the fact that these singularities are formally expected to be of order two, cf. the discussion in Section 4. The fact that the AAA algorithm works so well for branch points is analyzed in detail in a recent preprint by Lustri *et al.* [24]. Here, we observe similarly that for singularities which are close to poles of order two, the effective connection amplitude can be decomposed into a sum of connection amplitudes of the form (19), each associated with a simple pole, with high accuracy.

In this preliminary test, we have used the AAA algorithm on the entire time interval without restricting the number of interpolation nodes. The approximation is also done separately on the different components of the model, as in [45], which

leads to different locations of the poles, especially those further out in the complex plane, even though the location of singularities must be the same in all three components. In principle, this could be enforced by performing the optimization problem (28) simultaneously on the entire solution vector. In Section 6, however, we go a different route: we will use AAA approximation only on the z-component, cut the solution into small chunks, and put a hard limit on the number of poles.

Fig. 4 also shows the agreement with the horizontal location of the poles and the jumps in the fast energy of the forced oscillator (middle) and the correlation with the maxima of z (bottom).

We recall that, according to (22), the complex amplitude of the generated oscillation performs a discrete pseudo-random walk in the complex plane, with a step when a new Stokes line is crossed. Thus, the modulus of the fast amplitude increases maximally when the phase of the new connection amplitude is aligned with the current phase of the fast amplitude, it decreases maximally when the phases are anti-aligned but can do anything in between depending on the difference in phase. This is clearly visible in Fig. 4 where the big jumps require a pole relatively close to the real axis, but not every pole that is close to the real axis contributes a big jump. This sort of superposition is also discussed in the context of exponential asymptotics for nonlinear lattice waves in [10].

In a chaotic regime, pseudo-randomness of the continuous-time trajectories implies pseudo-randomness of the (discrete) sequence of singularities. Thus, we can use the AAA approximation of a Lorenz trajectory as a generator of either a pseudo-random or quasi-periodic sequence of complex conjugate pairs of poles.

6. Deterministic surrogate model

We now seek to replace the 5-dimensional dynamical system consisting of the Lorenz equations and the driven oscillator by a simpler one where only the slow dynamics are maintained as an ODE and the evolution of the fast amplitude is computed via the cumulative connection amplitude (22), where the terms are computed from the approximate discrete set of singularities of the z-component of the Lorenz system. The surrogate system is simpler not only because continuous-time dynamics is only three-dimensional but also, in particular, because it evolves only on the slow time scale. To solve the coupled 5-dimensional system, off-the-shelf time-stepping schemes would require time steps on the order of the fast period. This is prohibitive when ε is small. Of course, for this simple problem, there are various exponential time-stepping strategies that could maintain a time step uniform in ε. However, these need to be problem-adapted and do not generalize well.

Since we know that the singularities of the Lorenz system occur near the maxima of z and nowhere else, we can construct the surrogate model as follows.

(i) Take a (slow) numerical solution of the Lorenz model,
(ii) cut the discrete time series of the z-variable into pieces contained in intervals $[t_k^{\text{start}}, t_k^{\text{end}}]$ conditioned on the bound $z(t) \geq z_\star$,
(iii) feed the time series from each piece into the AAA algorithm limited to order $m \leq m_{\max}$ to obtain a list of poles and residues for each interval,
(iv) remove spurious poles, defined as poles whose real part lies outside of the interpolation interval $[t_k^{\text{start}}, t_k^{\text{end}}]$,

(v) compute the local complex connection amplitude

$$B_k = \frac{2\pi}{\varepsilon} \sum_{(a,z)\in\mathcal{P}} a\, \mathrm{e}^{\mathrm{i}z/\varepsilon}\,, \tag{29}$$

where $\mathcal{P}$ denotes the set of tuples (a, z) that characterize the remaining set of complex-conjugate pairs of poles, with a denoting the residue and z the location of the member of the pair that has $\operatorname{Im} z > 0$.

The global evolution of the fast amplitude is finally given by the cumulative connection formula (22).

To check whether the approximation of the change in fast amplitude via the local connection formula (29) is accurate, we first perform a pre-test in which we compare each B_k with a direct numerical solution as follows: We initialize the coupled model in a balanced state at each t_k^{start} via (4), evolve forward in time, and diagnose the fast amplitude as the square root of the fast energy (6) at t_k^{end}. Fig. 5 shows the resulting distribution of the relative error, where positive values indicate that the fast amplitude from direct numerical simulation is larger than B_k, and vice versa. The distribution is highly peaked within a band of about 0.5 %, but has a longer tail toward positive values. Thus, errors are small but far from negligible, with a non-zero mean.

We note that the error is not uniform as $\varepsilon \to 0$. The reason is that the AAA algorithm replaces the second-order branch point by a collection of poles that have close, but not identical real parts of their locations. Since these real parts determine the phase of the associated connection amplitude, they are coherent only so long as the period of the fast oscillation is long compared to the phase jitter introduced by the approximation. As $\varepsilon \to 0$, coherence will eventually be lost and the approximation degrades. This effect has been studied and explained in detail in a recent preprint [24]. Increasing the maximal number of poles will lead to better behavior for small values of ε. We conjecture that uniform-in-ε behavior can be obtained in our setting by modifying the AAA algorithm to force all poles to have the same real part.

We then let both models evolve freely. Fig. 6 compares the direct numerical simulation to the surrogate model, showing remarkably good agreement over a large number of events. To explain how this is possible, we first note that the coupled model and the surrogate model use the identical numerical trajectory for the Lorenz subsystem. Thus, the rapid exponential divergence of Lorenz trajectories is not at play here. However, if we were using even slightly different numerical settings for the two cases, we would see entirely different trajectories on the time scale shown.

Perhaps more surprising is the fact that when both models evolve freely, the agreement is much better than the amplitude error statistics shown in Fig. 5 would suggest. One reason is the following: When $B(k)$ is nonzero for some k, the effect of adding the next complex jump amplitude B_{k+1} to the current fast amplitude $B(k)$ depends on the relative phase between the two. Due to the scale separation, this relative phase is essentially random and uniformly distributed, so that the effect of the error in B_{k+1} on the new amplitude $|B(k+1)|$ is distributed nearly symmetrically about 0 when $|B(k)| \gg |B_{k+1}|$. Thus, the error in $B(k)$ can be considered as a random walk on top of the pseudo-random walk $B(k)$, thus grows like $\sqrt{k}$ in expectation, not like k as could be expected naively. However, even this explanation does not fully account for the remarkable long-time accuracy of the

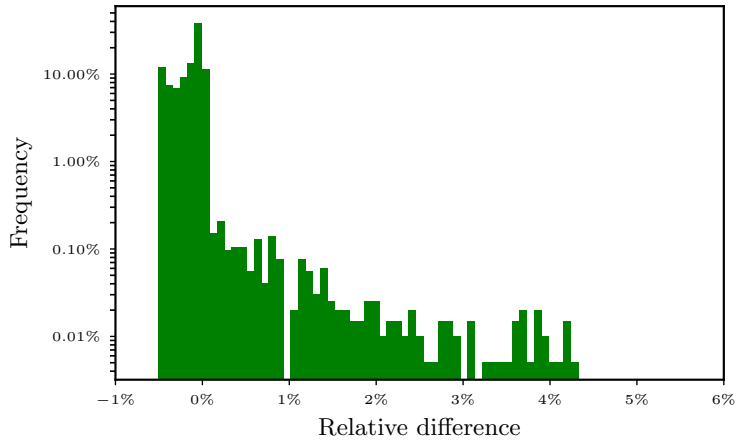

FIGURE 5. Distribution of the difference between the fast amplitude from direct numerical evaluation and the fast amplitude from the connection formula at time t_k^{end}, relative to the largest such amplitude, when the fast component is re-initialized to a balanced state at every t_k^{start}. The mean of this distribution is at a relative difference of $-0.15\,\%$.

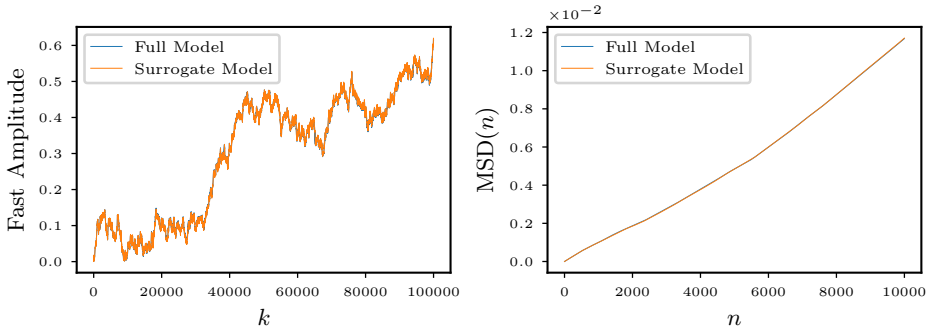

FIGURE 6. Comparison between the full model with the surrogate model in the chaotic regime for $\varepsilon = 0.01$. The two trajectories are visually almost identical over a time period covering 100 000 return events.

surrogate model. Numerically, we observe a strong remnant temporal correlation of the surrogate model error across neighboring jump events. The precise mechanism remains an open question.

As a key statistical measure we compute, inspired by the "0–1 test" described in Section 4, the finite-time mean square displacement

$$\mathrm{MSD}(n) = \sum_{j=1}^{N} \frac{|p_{j+n} - p_j|^2 + |q_{j+n} - q_j|^2}{N}\,, \tag{30}$$

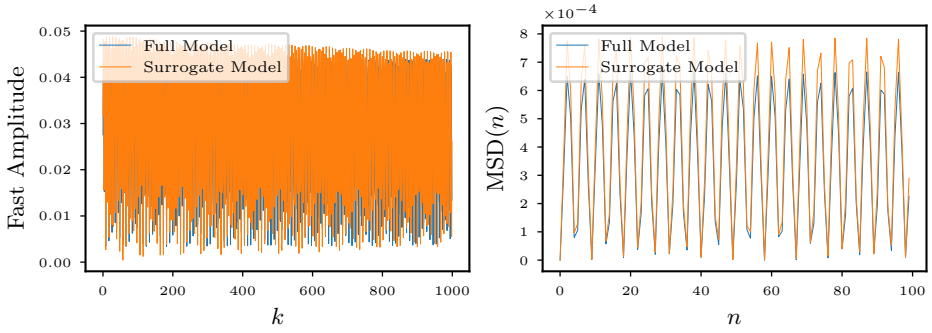

FIGURE 7. Comparison between the full model with the surrogate model in the periodic regime with $\varepsilon = 0.001$.

with $p_j = \varepsilon\, \dot{q}_{\text{fast}}(t_j^{\text{end}})$ and $q_j = q_{\text{fast}}(t_j^{\text{end}})$, where N is the number of z-excursions as separated out in Step (ii) above. As suggested in [19], we restrict to $n \leq N/10$; for larger values of n, the finite-time mean-square displacement will deviate significantly from its time-asymptotic value.

In a parameter regime where the Lorenz dynamics is periodic, the resulting fast amplitude is quasi-periodic, both for the full system and for the surrogate system (Fig. 7). Moreover, the MSD remains bounded, as expected from the "0–1 test", with only minor quantitative differences between the two models.

7. Stochastic surrogate model

Even though we have seen that the reconstruction of the full complex connection amplitude, including phase information, is remarkably successful, it may be too much to ask for from a modeling perspective. An $O(\varepsilon)$ perturbation to the state of the Lorenz system will cause an $O(1)$ change in phase for the connection amplitude already from one Stokes line event to the next. Thus, regarding the ability of the model to predict the future, the phase may be considered effectively random.

In the present setting, we can easily modify the connection formula by adding an independently uniformly distributed random phase to each term in the cumulative connection formula, defining

$$B_{\text{rand}}(m) = \sum_{i=1}^{m} B_i\, \mathrm{e}^{\mathrm{i}\alpha_k} \quad \text{with } \alpha \sim \mathcal{U}_{[0,2\pi]}\,. \tag{31}$$

Within the formula for the local connection amplitude (29), the phase must be kept coherent, as the set of local poles is merely an approximation to a single pair of branch points.

This stochastic surrogate model, of course, does not follow the development of the fast amplitude path-wise, but also has a linear growth of mean-square displacement in the chaotic regime, with approximately the same slope (Fig. 8). When the phase of the connection amplitude is randomized with periodic driving, the behavior of fast energy is statistically that of the fast energy in the chaotic driving regime (Fig. 9).

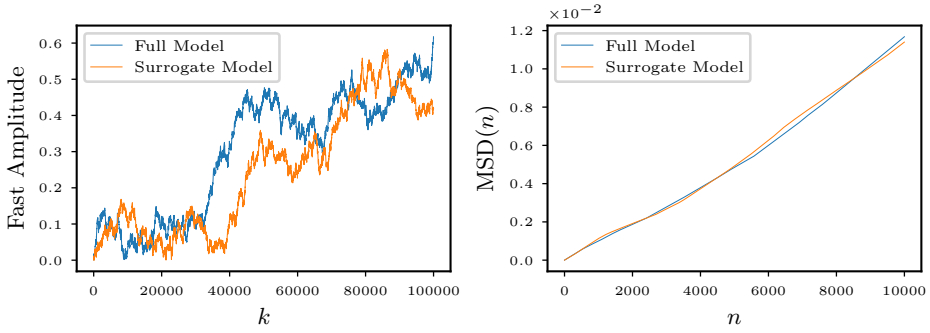

FIGURE 8. Comparison between the full model with the surrogate model with phase randomization in the chaotic regime, with $\varepsilon = 0.01$.

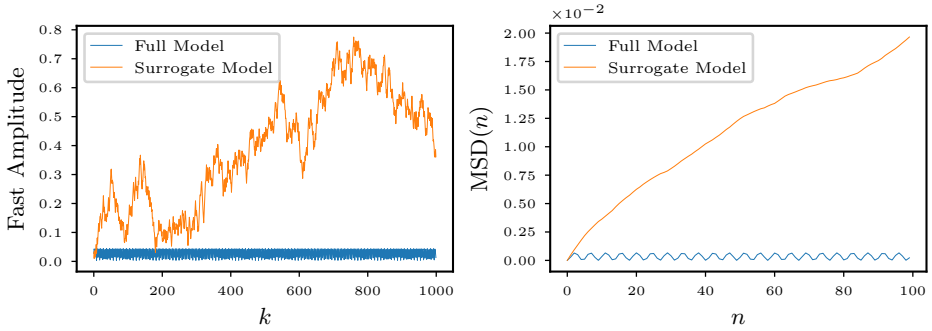

FIGURE 9. Comparison between the full model with the surrogate model with phase randomization in the periodic regime, with $\varepsilon = 0.001$.

8. Discussion

We have shown that the discrete structure of singularities in complex time of the forcing function suffices to describe the level of energy in a forced fast harmonic oscillator, locally with good accuracy and excellent long-time behavior due to the fact that local errors partially cancel over a long time scale. Thus, a discrete surrogate model that takes the singularity structure of the forcing function as input suffices to represent the evolution of fast energy with high accuracy.

The distance on the real axis between poles, linked to the relative phase of the contribution to the fast energy of each pole dictates whether or not an upcoming pole will contribute constructively or destructively. While this phase is uniformly distributed, for finite scale separation even a chaotic forcing signal has enough remnant phase correlations that they are visible in the long-time statistics of the evolution of the fast energy. Thus, complete randomization of the phase will underestimate the mean square displacement of the fast amplitude (or energy).

We further observed that the long-time behavior of the fast energy of a forced harmonic oscillator can be used to detect whether the forcing signal is chaotic or

not, in complete analogy with the "0–1 test for chaos" [17, 19]. More generally, this work gives an example of how even exponentially small phenomena can accrue significant contributions over a large number of events, which means that they may not be negligible and must be modeled.

So far, we have explored one of the simplest possible settings. We believe that it will be easy to extend these ideas to related low-dimensional systems where a connection formula is known, such as those considered in [39, 40, 42]. Alternative approaches for low-dimensional models based on machine learning have, e.g., been developed in [7].

More challenging is the extension to the geophysical balance problem where the setting is infinite-dimensional and where it is not even clear whether global linear wave and vortical modes are the right basis in which to describe the problem. In addition, there may be nonlinear fast-fast interactions which imply that the simple linear superposition of the contribution of each pole does not strictly hold true (see the discussion in [24]). Nonetheless, we conjecture that the linear growth of the mean square displacement of the amplitude of the fast degree of freedom seen here generalizes to the linear growth of mean square displacement of inertial gravity wave amplitudes in geophysical flows forced by turbulent eddy fields. This type of "spontaneous generation" of waves may therefore provide a non-negligible contribution to the energy cycle worth further study.

Acknowledgments

We thank Mickaël Chekroun, Sergey Danilov, Georg Gottwald, Stephan Juricke, Edgar Knobloch, Anton Kutsenko, Nick Trefethen, Jacques Vanneste, and Nedjeljka Žagar for stimulating discussions and remarks on various aspects of this work. We further thank the anonymous referees for insightful comments and the suggestion of further highly relevant references. Our numerical experiments use the implementation of the AAA algorithm by Clemens Hofreither [20, 21] which we gratefully acknowledge. This paper is a contribution to project L2 of the Collaborative Research Center TRR 181 "Energy Transfers in Atmosphere and Ocean" funded by the Deutsche Forschungsgemeinschaft (DFG, German Research Foundation) under project number 274762653.

References

[1] M. Abramowitz and I. A. Stegun, eds., *Handbook of Mathematical Functions with Formulas, Graphs, and Mathematical Tables*, United States National Bureau of Standards, Washington, DC, USA, 1972.

[2] A. J. Alvarez-Socorro, M. G. Clerc, M. A. Ferré, and E. Knobloch, *Front depinning by deterministic and stochastic fluctuations: a comparison*, Phys. Rev. E, 99 (2019), pp. 062226, 11.

[3] A. C. Antoulas and B. D. Q. Anderson, *On the scalar rational interpolation problem*, IMA J. Math. Control Inform., 3 (1986), pp. 61–88.

[4] J.-P. Berrut, *Rational functions for guaranteed and experimentally well-conditioned global interpolation*, Comput. Math. Appl., 15 (1988), pp. 1–16.

[5] J.-P. Berrut and L. N. Trefethen, *Barycentric Lagrange interpolation*, SIAM Rev., 46 (2004), pp. 501–517.

[6] M. V. Berry, *Stokes' phenomenon; smoothing a Victorian discontinuity*, Inst. Hautes Études Sci. Publ. Math., (1988), pp. 211–221.

[7] M. D. Chekroun, H. Liu, and J. C. McWilliams, *Stochastic rectification of fast oscillations on slow manifold closures*, Proc. Natl. Acad. Sci. USA, 118 (2021), pp. Paper No. e2113650118, 9.

[8] C. J. Cotter and S. Reich, *Semigeostrophic particle motion and exponentially accurate normal forms*, Multiscale Model. Sim., 5 (2006), pp. 476–496.
[9] S. M. Cox and A. J. Roberts, *Initialization and the quasi-geostrophic slow manifold*, arXiv:nlin/0303011, (2003).
[10] G. Deng and C. J. Lustri, *Exponential asymptotics of woodpile chain nanoptera using numerical analytic continuation*, Stud. Appl. Math., 150 (2023), pp. 520–557.
[11] R. B. Dingle, *Asymptotic expansions: their derivation and interpretation*, Academic Press, London-New York, 1973.
[12] H. R. Dullin, S. Schmidt, P. H. Richter, and S. K. Grossmann, *Extended phase diagram of the Lorenz model*, Internat. J. Bifur. Chaos Appl. Sci. Engrg., 17 (2007), pp. 3013–3033.
[13] M. S. Floater and K. Hormann, *Barycentric rational interpolation with no poles and high rates of approximation*, Numer. Math., 107 (2007), pp. 315–331.
[14] C. Foias, M. S. Jolly, I. Kukavica, and E. S. Titi, *The Lorenz equation as a metaphor for the Navier-Stokes equations*, Discrete Contin. Dynam. Systems, 7 (2001), pp. 403–429.
[15] V. Gelfreich and L. Lerman, *Almost invariant elliptic manifold in a singularly perturbed Hamiltonian system*, Nonlinearity, 15 (2002), pp. 447–457.
[16] ———, *Long-periodic orbits and invariant tori in a singularly perturbed Hamiltonian system*, Phys. D, 176 (2003), pp. 125–146.
[17] G. A. Gottwald and I. Melbourne, *A new test for chaos in deterministic systems*, Proc. R. Soc. Lond. Ser. A Math. Phys. Eng. Sci., 460 (2004), pp. 603–611.
[18] ———, *On the validity of the* 0–1 *test for chaos*, Nonlinearity, 22 (2009), pp. 1367–1382.
[19] ———, *The* 0–1 *test for chaos: A review*, in Chaos, Detection, and Predictability, C. H. Skokos, G. A. Gottwald, and J. Laskar, eds., Springer, Berlin, Heidelberg, 2016, pp. 221–247.
[20] C. Hofreither, *An algorithm for best rational approximation based on barycentric rational interpolation*, Numer. Algorithms, 88 (2021), pp. 365–388.
[21] ———, *baryrat: Barycentric rational approximation*, 2022. GitHub repository, GitHub, commit 3c19a91, https://github.com/c-f-h/baryrat.
[22] G. Klein, *Applications of linear barycentric rational interpolation*, PhD thesis, Université de Fribourg, 2012.
[23] E. N. Lorenz, *Deterministic Nonperiodic Flow*, J. Atmos. Sci., 20 (1963), pp. 130–141.
[24] C. J. Lustri, S. C. Crew, and S. J. Chapman, *Exponential asymptotics using numerical rational approximation in linear differential equations*, arXiv, 2312.07773 (2023).
[25] R. S. MacKay, *Slow manifolds*, in Energy Localisation and Transfer, T. Dauxois, A. Litvak-Hinenzon, R. S. MacKay, and A. Spanoudaki, eds., World Scientific, Singapore, 2004, pp. 149–192.
[26] M. McIntyre, *Dynamical meteorology – balanced flow*, in Encyclopedia of Atmospheric Sciences, J. Pyle and F. Zhang, eds., Academic Press, Oxford, second ed., 2015, pp. 298–303.
[27] Y. Nakatsukasa, O. Sète, and L. N. Trefethen, *The AAA algorithm for rational approximation*, SIAM J. Sci. Comput., 40 (2018), pp. A1494–A1522.
[28] ———, *The first five years of the AAA algorithm*, arXiv, 2312.03565 (2023).
[29] A. Neishtadt, *Averaging method and adiabatic invariants*, in Hamiltonian dynamical systems and applications, NATO Sci. Peace Secur. Ser. B Phys. Biophys., Springer, Dordrecht, 2008, pp. 53–66.
[30] A. I. Neĭshtadt, *The separation of motions in systems with rapidly rotating phase*, Prikl. Mat. Mekh., 48 (1984), pp. 197–204.
[31] N. Nekhoroshev, *An exponential estimate of the time of stability of a nearly-integrable Hamiltonian system*, Russ. Math. Surv., 32 (1977), pp. 1–65.
[32] A. B. Olde Daalhuis, S. J. Chapman, J. R. King, J. R. Ockendon, and R. H. Tew, *Stokes phenomenon and matched asymptotic expansions*, SIAM J. Appl. Math., 55 (1995), pp. 1469–1483.
[33] H. E. Salzer, *Rational interpolation using incomplete barycentric forms*, Z. Angew. Math. Mech., 61 (1981), pp. 161–164.
[34] C. Schneider and W. Werner, *Some new aspects of rational interpolation*, Math. Comp., 47 (1986), pp. 285–299.
[35] R. Temam and D. Wirosoetisno, *Exponential approximations for the primitive equations of the ocean*, Discrete Contin. Dyn. Syst. Ser. B, 7 (2007), pp. 425–440.
[36] L. N. Trefethen, *Quantifying the ill-conditioning of analytic continuation*, BIT, 60 (2020), pp. 901–915.

[37] L. N. Trefethen, *Numerical analytic continuation*, Japan J. Indust. Appl. Math., (2023), pp. 1–50.
[38] L. N. Trefethen, Y. Nakatsukasa, and J. A. C. Weideman, *Exponential node clustering at singularities for rational approximation, quadrature, and PDEs*, Numer. Math., 147 (2021), pp. 227–254.
[39] J. Vanneste, *Inertia-gravity wave generation by balanced motion: revisiting the Lorenz-Krishnamurthy model*, J. Atmospheric Sci., 61 (2004), pp. 224–234.
[40] ———, *Exponential smallness of inertia–gravity wave generation at small Rossby number*, J. Atmos. Sci., 65 (2008), pp. 1622–1637.
[41] J. Vanneste, *Balance and spontaneous wave generation in geophysical flows*, Ann. Rev. Fluid Mech., 45 (2013), pp. 147–172.
[42] J. Vanneste and I. Yavneh, *Exponentially small inertia–gravity waves and the breakdown of quasigeostrophic balance*, J. Atmos. Sci., 61 (2004), pp. 211–223.
[43] D. Viswanath and S. Şahutoğlu, *Complex singularities and the Lorenz attractor*, SIAM Rev., 52 (2010), pp. 294–314.
[44] T. Warn, O. Bokhove, T. Shepherd, and G. Vallis, *Rossby number expansions, slaving principles, and balance dynamics*, Quart. J. R. Meteorol. Soc., 121 (1995), pp. 723–739.
[45] M. Webb, *Computing complex singularities of differential equations with Chebfun*, SIAM Undergrad. Res. Online, 6 (2013), pp. 130–151.

(M. Oliver and M. Tiofack Kenfack) Mathematical Institute for Machine Learning and Data Science, KU Eichstätt–Ingolstadt, 85049 Ingolstadt, Germany

(M. Oliver) Constructor University, 28759 Bremen, Germany